Resonance cones in cold plasma: origin, singularities, and power flow

W. Tierens,[1] F. Paulus,[2] and R. Bilato[2]
[1)]*Oak Ridge National Laboratory, 1 Bethel Valley Road, Oak Ridge, TN 37830, USA*
[2)]*Max Planck Institute of Plasma Physics, Boltzmannstraße 2, 85748 Garching, Germany*

(*Electronic mail: tierenswv@ornl.gov)

(Dated: 11 October 2023)

In magnetized tenuous plasma, typical at the plasma edge of fusion devices, a nearly electrostatic wave mode with relatively enhanced electric field can propagate along a specific angle with the magnetic field. For this characteristic, it is known as a "resonance cone". For instance, these waves can be excited by radio-frequency antennas in the ion-cyclotron and lower-hybrid range of frequencies. We consider the resonance cones emitted by idealized spatially extended sources. In 2D, we use a novel geometric construction which generalizes the d'Alembert solution to curved boundaries / moving sources, and show, for the first time, that singular electric fields arise under these conditions, thereby bringing the resonance cones in line with the other resonances of the cold plasma theory. Still in 2D, we give an expression for the amount of power radiated by resonance cones in terms of surface quantities on the source, which is finite despite the singular electric field. We generalize the conclusions regarding the presence and location of singular electric fields to the 3D electromagnetic case.

I. INTRODUCTION

In the cold plasma approximation, which is typically justified in the edge of current and future tokamaks, the electromagnetic properties of the medium are given by the dielectric tensor[1]

$$\varepsilon = \begin{bmatrix} S & iD & 0 \\ -iD & S & 0 \\ 0 & 0 & P \end{bmatrix} \tag{1}$$

in Cartesian coordinates with the confining magnetic field along the z axis, using the conventional Stix notation[1],

$$S = 1 - \frac{1}{2}\sum_s \frac{\omega_s^2}{\omega(\omega+\Omega_s)} - \frac{1}{2}\sum_s \frac{\omega_s^2}{\omega(\omega-\Omega_s)} \tag{2}$$

$$P = 1 - \sum_s \frac{\omega_s^2}{\omega^2} \tag{3}$$

where ω_s, Ω_s are the plasma resp. cyclotron frequency of particle species s. D will not be needed in this work.

The complex frequency-domain electromagnetic fields in this medium are solutions of the frequency-domain wave equation

$$\nabla \times \nabla \times \boldsymbol{E} - k_0^2 \varepsilon \boldsymbol{E} = 0 \tag{4}$$

If the signs of S and P differ, a nearly electrostatic short-wavelength wave mode propagates at a specific angle with the magnetic field, a wave whose phase and group velocities are orthogonal. According to the classical derivation[2], we assume a homogeneous plasma, an electrostatic electric field $\boldsymbol{E} = -\nabla\phi$, and set $\nabla \cdot \boldsymbol{D} = \nabla \cdot \varepsilon \boldsymbol{E} = 0$, yielding

$$\frac{\partial^2}{\partial_z^2}\phi = \frac{-S}{P}\left(\frac{\partial^2}{\partial_x^2} + \frac{\partial^2}{\partial_y^2}\right)\phi \tag{5}$$

(5) describes only the nearly electrostatic "slow wave" mode from (4), neglecting the other mode, the "fast wave", which is also described by (4). (5) is, formally, a 2D time-domain wave equation, with z (the direction along the magnetic field) playing the role of the time direction, and the positive quantity $\sqrt{-S/P}$ playing the role of the wave propagation speed. This formal analogy makes it immediately clear why cone-like structures form in the electromagnetic field pattern.

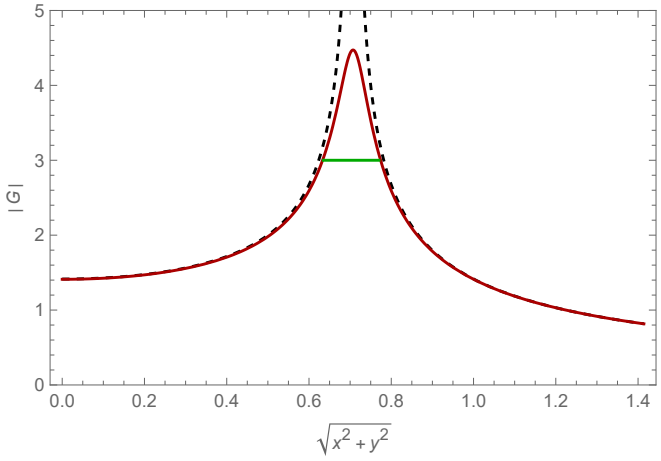

FIG. 1. Introducing collision-like losses in cold plasma by making S and P complex, removes the singularity in the Green's function $G \propto 1/\sqrt{\frac{-S}{P}z^2 - x^2 - y^2}$ (Red curve: collisional, black dashed: collisionless), yielding a cone with a well-defined finite thickness. Parameters are: $S = 1, P = -2, z = 1$, and $S = 1 + i/10$ for the collisional case.

This paper deals with solutions of (5) in the presence of smooth, extended, non-singular sources, going beyond the existing literature which is limited to the case of singular point sources.

This paper is organized as follows: section II discusses the Green's functions of (5), the divergence of which is usually identified with the "resonance cone". Section III considers the electrostatic description for 2D extended sources (as opposed to the point sources that give rise to the Green's func-

tions), and shows that there is still a field singularity, emitted from specific points on the source surface. We also give a new physical interpretation of those emission points in the context of (5) as a time-domain wave equation. In section IV we return to the electromagnetic case, in 2D and 3D, and reach the same conclusion w.r.t. the existence and location of the emission points of singular electric fields on the source surface. The conclusion is in section V.

II. GREEN'S FUNCTIONS FOR EQUATION (5)

The classical derivation[2] proceeds by constructing a Green's function for (5)

$$G \propto \frac{1}{\sqrt{\frac{-S}{P}z^2 - x^2 - y^2}} \tag{6}$$

which is shown in figure 1. The boundary conditions that specify (6) are the presence of a time-oscillating point charge $\nabla \cdot \boldsymbol{D} = \delta(x,y,z)$ and the potential approaches zero at infinity $\lim_{(x,y,z)\to\infty} G = 0$. Neither condition gives us any guarantees about the behavior of the Poynting vector of the electromagnetic phenomenon of which $\boldsymbol{E} = -\nabla\phi$ is a mere electrostatic approximation. We will revisit this point in section III J.

Both G and ∇G diverge along the cone $Px^2 + Py^2 = -Sz^2$, which Bellan[2] defines as the "resonance cone". Brambilla[3] reaches the same conclusion, that the electric field emitted by a point source diverges along a cone, without using the electrostatic approximation.

In this work, we will show for the first time that singular electric fields arise along the resonance cone even for extended sources, even in the absence of singular charge densities at the source. As such, we are interested in other Green's function for the time-domain wave equation (5), the classical one being

$$G \propto \frac{1}{\sqrt{\frac{-S}{P}z^2 - x^2 - y^2}} \Theta\left(\sqrt{\frac{-S}{P}}z - \sqrt{x^2+y^2}\right) \tag{7}$$

which is specified by the boundary conditions $\phi(x,y,z=0) = \delta(x,y)$ and $\partial_z\phi(x,y,z=0) = 0$. The time-domain causality is readily apparent in the Heaviside step function Θ which is not present in (6): the time-symmetry (z-symmetry) of (5) must be deliberately broken when we solve it as a time-domain wave equation. For the resonance cone, on the other hand, that symmetry is manifest: these cones propagate in both directions along the magnetic field. Thus, we must at least restore z-symmetry

$$G \propto \frac{1}{\sqrt{\frac{-S}{P}z^2 - x^2 - y^2}} \Theta\left(\sqrt{\frac{-S}{P}}|z| - \sqrt{x^2+y^2}\right) \tag{8}$$

In the 2D case, with $\partial/\partial_y = 0$, (5) becomes

$$\frac{\partial^2}{\partial_z^2}\phi = \frac{-S}{P}\frac{\partial^2}{\partial_x^2}\phi \tag{9}$$

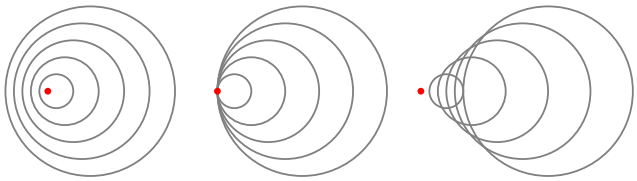

FIG. 2. Pressure waves, such as those modeled by the same time-domain wave equation (5) that also describes the potential of the resonance cone in the electrostatic limit, emitted by a source moving to the left, visualized in the frame in which the medium is stationary. When the source moves at the speed of sound, these waves exhibit an "infinite pressure gradient" where the wave fronts bunch up arbitrarily closely.

The 2D Green's functions

$$G_0 = \delta(x-cz) + \delta(x+cz) \tag{10}$$
$$cG_1 = \Theta(x+cz) - \Theta(x-cz) \tag{11}$$

give rise to the classical d'Alembert solution of (9)

$$2\phi(x,z) = \phi_0(x-cz) + \phi_0(x+cz) + \frac{1}{c}\int_{x-cz}^{x+cz}\phi_1(s)ds \tag{12}$$

where $c = \sqrt{-S/P}$ is the wave speed and $\phi(x,0) = \phi_0(x)$ and $\frac{\partial}{\partial z}\phi(x,0) = \phi_1(x)$ are the boundary conditions at $z = 0$. For any regular initial conditions $\phi_0(x), \phi_1(x)$, we obtain a regular solution for all z. If both $\phi_0(x), \phi_1(x)$ and $d\phi_0/dx, d\phi_1/dx$ are regular, the resulting potential $\phi(x,z)$ and electric field $-\nabla\phi(x,z)$ are regular. Indeed, this is what Myra[4] found: an extended source, imposed as a smooth boundary condition along a coordinate plane, emits a cone whose electric field remains finite throughout. In that scenario, no physical quantities diverge, and no collisions are needed to regularize the solution, in stark contrast with other resonances known in cold plasma theory[5,6].

III. EXTENDED SOURCES IN THE 2D ELECTROSTATIC CASE

A. A guiding example

Consider a circle with radius r_s as a source surface. Consider

$$f(x) = \sqrt{1 - \frac{x^2}{r_s^2(1+c^2)}}\,\Theta\left(1 - \frac{x^2}{r_s^2(1+c^2)}\right) \tag{13}$$
$$\phi = f(x+cz) + f(x-cz) \tag{14}$$

where Θ is the Heaviside step function. The reader may verify that this ϕ has the following properties, which we will explore in more generality later:

- ϕ is a solution of (9).
- ϕ is continuous and finite.

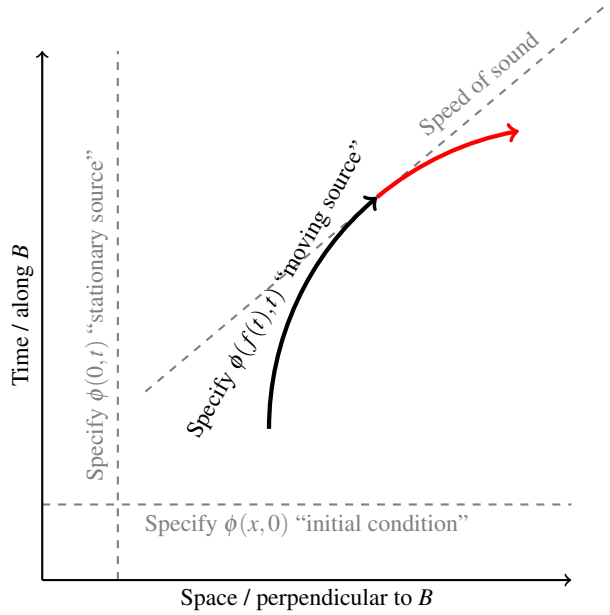

FIG. 3. Three kinds of boundary conditions of the time-domain wave equation (9). The initial conditions at constant t or stationary sources at constant x are the most common, but here we must consider a moving source, which may cross the speed of sound (black: subsonic, red: supersonic). It is always necessary to specify two boundary conditions to uniquely specify a solution of this second-order PDE, e.g. the d'Alembert solution (12) specifies both the value and the time-derivative along a line of constant t.

- The component of $\boldsymbol{E} = -\nabla\phi$ tangential to the circle is finite.
- The component of $\boldsymbol{D} = -\varepsilon_0\varepsilon\nabla\phi$ normal to the circle is finite.
- The component of $\boldsymbol{E} = -\nabla\phi$ normal to the $r = r_s$ circle is singular at the roots of $S\cos^2(\theta) + P\sin^2(\theta) = 0$. This singularity remains along the lines tangent to the circle at those points.

B. Breaking the sound barrier

A general 2D source is a boundary condition imposed along some (usually closed) curve in the x-z plane. Equation (9), interpreted again as a 1D time-domain wave equation with z playing the role of the time direction, offers a physical interpretation of the resonance cones emitted in this scenario: they correspond to the case of a *moving* source. We expect, and we will indeed find, peculiar behavior when the source "moves" at the "wave speed" c (figures 2 and 3), behavior that would not be observed when the source is imposed along a coordinate plane.

Let us consider this precise analogy in some detail. Using the Green's functions (10) and (11) we will construct generic solutions of (9) in the presence of a cylindrical (circular) source of radius r_s. The same construction works for any convex source, and can be seen as a generalization of the d'Alembert solution. Before we can proceed with this construction, let us introduce some geometry.

C. Geometry

Let θ_i, $i = 1,\cdots,4$ be the four roots of $S\cos^2(\theta_i) + P\sin^2(\theta_i) = 0$:

$$\theta_1 = \arctan(c) \tag{15}$$
$$\theta_2 = \pi - \arctan(c) \tag{16}$$
$$\theta_3 = \arctan(c) - \pi \tag{17}$$
$$\theta_4 = -\arctan(c) \tag{18}$$

The points $T_i = (r_s\cos(\theta_i), r_s\sin(\theta_i))$ are where the source crosses the speed of sound in the view of figure 3. Let L_i be the line tangent to the source circle at T_i, which we parameterize as follows:

$$L_i(\delta) = T_i + (-\sin(\theta_i), \cos(\theta_i))\delta \tag{19}$$

let $L_\pm(x,z)$ be the line that passes through the point (x,z) and has slope $\pm 1/c$ (these lines being the characteristics of (9)). Consider the points where the source circle intersects the line $L_\pm(x,z)$. Let $P_\pm(x,z)$ be the closest of these intersection points to (x,z), if the intersection exists, or the closest point on the circle to $L_\pm(x,z)$, if no intersection exists. Figures 4 and 5 clarify this definition. Let $\theta_\pm(x,z)$ be the azimuthal coordinate of $P_\pm(x,z)$ expressed in polar coordinates $(x,z) = (r\cos(\theta), r\sin(\theta))$.

Let $\xi_+ = (x,z)\cdot(\cos(\theta_2),\sin(\theta_2))$ and $\xi_- = (x,z)\cdot(\cos(\theta_1),\sin(\theta_1))$, coordinates normal to the characteristics of (9). The lines $L_\pm$ are lines of constant $\xi_\pm$.

Explicit expressions for $\theta_\pm(x,z)$ are

$$\theta_-(x,z)=\begin{cases}\arctan(c) & \xi_->r_s\\ \arctan(c)-\pi & \xi_-<-r_s\\ \arctan\left(\xi_- - c\sqrt{r_s^2-\xi_-^2}, c\xi_- + \sqrt{r_s^2-\xi_-^2}\right) & \xi_-\in[-r_s,r_s]\wedge\xi_+(c^2+1)>\xi_-(c^2-1)\\ \arctan\left(c\sqrt{r_s^2-\xi_-^2}+\xi_-, c\xi_- - \sqrt{r_s^2-\xi_-^2}\right) & \text{Otherwise}\end{cases} \tag{20}$$

$$\theta_+(x,z)=\begin{cases}\pi-\arctan(c) & \xi_+>r_s\\ -\arctan(c) & \xi_+<-r_s\\ \arctan\left(-c\sqrt{r_s^2-\xi_+^2}-\xi_+, c\xi_+ - \sqrt{r_s^2-\xi_+^2}\right) & \xi_+\in[-r_s,r_s]\wedge\xi_-(c^2+1)<\xi_+(c^2-1)\\ \arctan\left(c\sqrt{r_s^2-\xi_+^2}-\xi_+, c\xi_+ + \sqrt{r_s^2-\xi_+^2}\right) & \text{Otherwise}\end{cases} \tag{21}$$

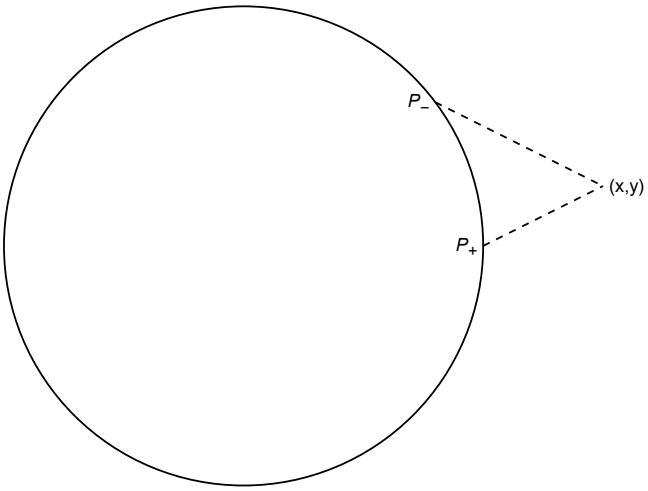

FIG. 4. Definition of $P_\pm(x,z)$: if the intersection between the source circle and the line $L_\pm(x,z)$ (which passes through (x,z) and has slope $\pm 1/c$) exists, $P_\pm(x,z)$ is the closest of these intersections to (x,y).

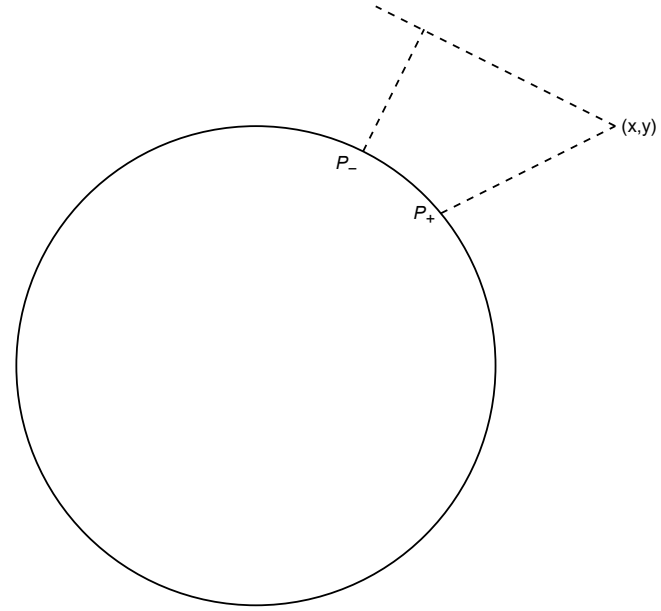

FIG. 5. Definition of $P_\pm(x,z)$: if the intersection between the source circle and the line $L_\pm(x,z)$ (which passes through (x,z) and has slope $\pm 1/c$) does not exist, $P_\pm(x,z)$ is the point on the circle closest to that line.

where $\arctan(x,y)$ is the usual two-parameter generalisation of the arctan function, such that $\arctan(x,y)=\arctan(y/x)$ for points in the first quadrant. The following series expansion will be useful to evaluate normal derivatives

$$\theta_\mp((r_s+\delta)\cos(\theta),(r_s+\delta)\sin(\theta)) = \theta \pm \frac{\delta(c\sin(\theta)\pm\cos(\theta))}{r_s(c\cos(\theta)\mp\sin(\theta))}+O(\delta^2) \tag{22}$$

Note that $\theta_\pm(x,z)$ depends exclusively on $\xi_\pm$ (there is a switch from one kind of dependence on $\xi_\pm$ to another kind of dependence on $\xi_\pm$, which depends on $\xi_\mp$, but that switch happens inside the cylinder, outside of the solution domain). Since general solutions of (9) have the form $f(\xi_+)+g(\xi_-)$ (because of the hole in our solution domain we will end up with solutions that can be locally, but not globally, decomposed like this), we will now consider solutions of the form $f(\theta_+)+f(\theta_-)$ in section III D, and solutions of the form $f(\theta_+)-f(\theta_-)$ in section III F.

D. Solution for a given azimuthal electric field and zero surface charge

Consider the following two boundary conditions: zero surface charge ($D_n=0$), and a given azimuthal electric field:

$$\frac{-1}{r_s}\frac{\partial}{\partial\theta}\phi(r_s\cos(\theta),r_s\sin(\theta))=f(\theta) \tag{23}$$

Let $\Phi_0(\theta)$ be an antiderivative of $-r_s f(\theta)$. Then, we have the following solution

$$2\phi_0(x,z)=\Phi_0(\theta_+(x,z))+\Phi_0(\theta_-(x,z)) \tag{24}$$

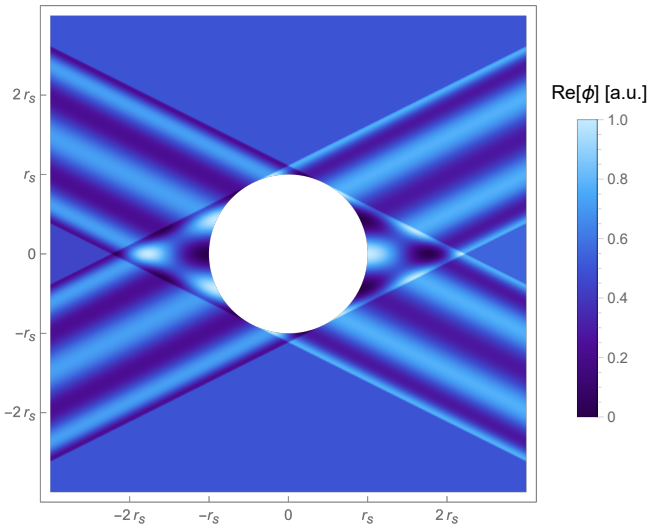

FIG. 6. Plot of (29) with $m = 7$, an exact solution, in the electrostatic approximation, of the potential ϕ whose gradient is the electric field of the resonance cone emitted by a cylindrical source in 2D. Parameters are $r_s = 1$mm (note the scale-invariance), $c = \sqrt{-S/P} = 2$.

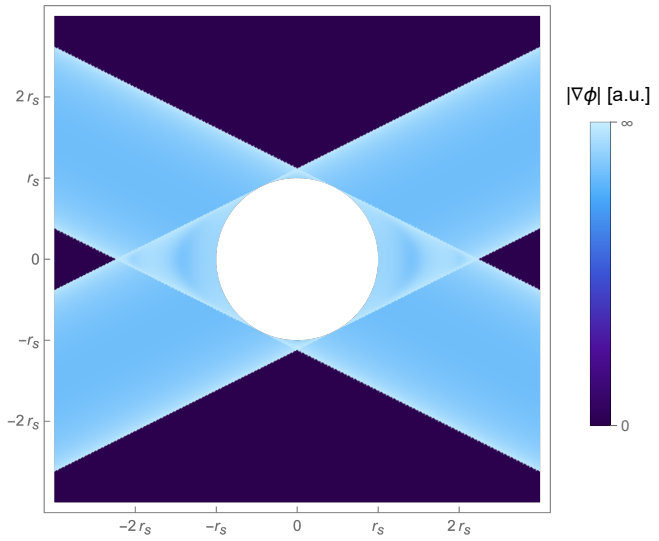

FIG. 7. Plot of $|\nabla\phi|$, the norm of the gradient of the potential from figure 6. The color scale is according to $\arctan(|\nabla\phi|)$.

Obviously,

$$\phi_0(r_s\cos(\theta), r_s\sin(\theta)) = \Phi_0(\theta) \tag{25}$$

$$\frac{-1}{r_s}\frac{\partial}{\partial\theta}\phi_0(r_s\cos(\theta), r_s\sin(\theta)) = f(\theta) \tag{26}$$

so ϕ_0 obeys the desired azimuthal electric field boundary condition. Using (22), we find the normal electric field

$$e_n = \frac{\left(c^2+1\right)\sin(2\theta)f(\theta)}{2\left(c^2\cos^2(\theta)-\sin^2(\theta)\right)} \tag{27}$$

Note the factor $c^2\cos^2(\theta) - \sin^2(\theta)$ in the denominator, which relates again to "crossing the speed of sound" in figure 3. The condition for D_n being zero is

$$e_n = \frac{\left(c^2+1\right)\sin(2\theta)}{2\left(c^2\cos^2(\theta)-\sin^2(\theta)\right)}e_\theta \tag{28}$$

which (27) indeed obeys.

E. Expansion of the first kind of solution into azimuthal modes

For $e_\theta = \exp(im\theta)$, $m \neq 0$ along the source surface, the solution is

$$\phi_0 = \frac{ir_s}{2m}\left(\exp(i\theta_+(x,z)m) + \exp(i\theta_-(x,z)m)\right) \tag{29}$$

Figure 6 shows this potential for $m = 7$, and figure 7 shows its gradient. There is no solution for $m = 0$, $e_\theta =$ constant, because that cannot be the gradient of a potential.

F. Solution for a given surface charge and zero azimuthal electric field

A second solution is

$$\phi_1(x,z) = \frac{-r_s}{2\varepsilon_0 cP}\int_{\theta_+(x,z)}^{\theta_-(x,z)} D_n(\theta)d\theta \tag{30}$$

where we integrate along the short arc from $\theta_+(x,z)$ to $\theta_-(x,z)$. ϕ_1 is zero along the source boundary, because $[\theta_+(x,z), \theta_-(x,z)]$ approaches the empty interval as (x,z) approaches the boundary. Hence, the azimuthal electric field vanishes along the boundary. For the normal electric field, the radial derivatives of $\theta_\pm$ are in (22), hence

$$\begin{aligned} e_n &= \left(\frac{-D_n(\theta)}{2\varepsilon_0 cP}\right)\left(\frac{c\sin(\theta)+\cos(\theta)}{c\cos(\theta)-\sin(\theta)} + \frac{c\sin(\theta)-\cos(\theta)}{c\cos(\theta)+\sin(\theta)}\right) \\ &= \left(\frac{-D_n(\theta)}{\varepsilon_0 P}\right)\frac{1}{c^2\cos^2(\theta)-\sin^2(\theta)} \\ &= \left(\frac{D_n(\theta)}{\varepsilon_0}\right)\frac{1}{S\cos^2(\theta)+P\sin^2(\theta)} \end{aligned} \tag{31}$$

Note again the factor $c^2\cos^2(\theta) - \sin^2(\theta)$ in the denominator, the same as in (27). Inserting this $e_n(\theta)$ into the expression for the surface charge density gives

$$\begin{aligned} &\begin{bmatrix}\cos(\theta)\\0\\\sin(\theta)\end{bmatrix}^T \varepsilon_0 \begin{bmatrix}S & iD & 0\\-iD & S & 0\\0 & 0 & P\end{bmatrix}\begin{bmatrix}\cos(\theta)\\0\\\sin(\theta)\end{bmatrix} e_n(\theta) \\ &\qquad = (S\cos^2(\theta)+P\sin^2(\theta))\varepsilon_0 e_n(\theta) \\ &\qquad = D_n(\theta) \end{aligned} \tag{32}$$

which confirms that this solution has the specified D_n.

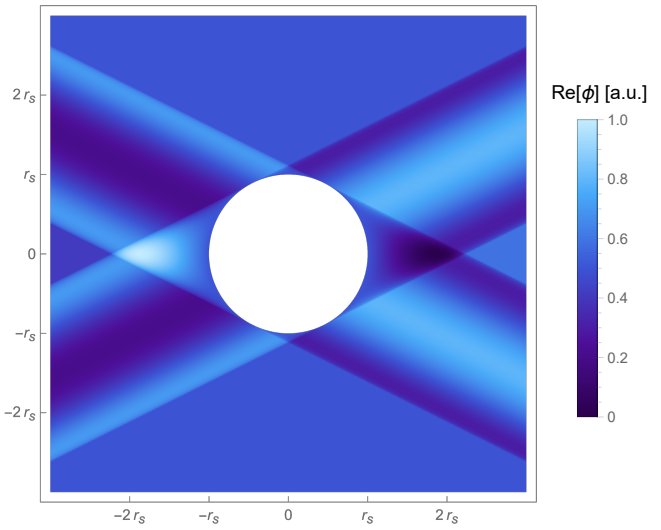

FIG. 8. Plot of (33) with $m = 3$, a second kind of exact solution, in the electrostatic approximation, of the potential ϕ whose gradient is the electric field of the resonance cone emitted by a cylindrical source in 2D. Parameters are $r_s = 1$mm (note the scale-invariance), $c = \sqrt{-S/P} = 2$.

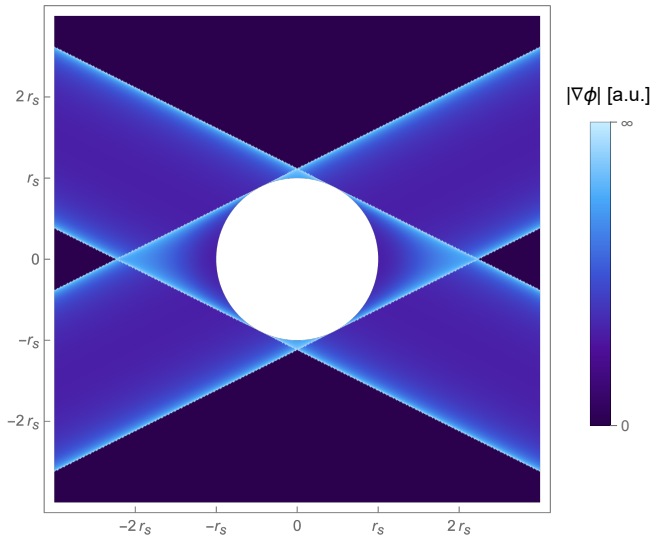

FIG. 9. Plot of $|\nabla\phi|$, the gradient of the potential from figure 8. The color scale is according to $\arctan(|\nabla\phi|)$

G. Expansion of the second kind of solution into azimuthal modes

For $D_n(\theta) = \exp(im\theta), m \neq 0$, the solution (30) becomes

$$\phi_1(x,z) = \frac{r_s}{2\varepsilon_0 cP}\frac{i\left(\exp(i\theta_- m) - \exp(i\theta_+ m)\right)}{m} \tag{33}$$

Figure 8 shows this potential for $m = 3$, and figure 9 shows its gradient.

For this second kind of solution, the $m = 0$ mode does exist. To calculate it, we may interpret $r_s \int_{\theta_+(x,z)}^{\theta_-(x,z)} 1 d\theta$ purely geometrically: it represents the length of the *short* arc from θ_+ to θ_-, positive if this arc is counterclockwise, negative if it is clockwise. This potential is in figure 10.

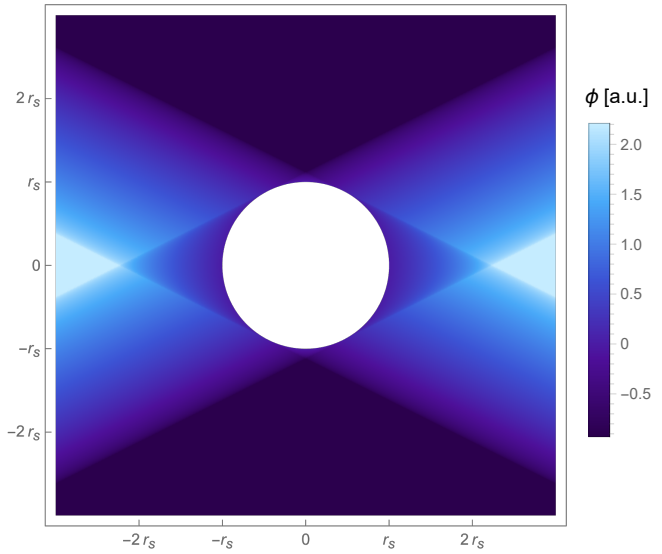

FIG. 10. The potential with $D_n =$ constant, the only solution with an $m = 0$ mode on the surface.

H. Presence of singular gradients in both kinds of solution

Both kinds of solution exhibit divergent gradients along the lines L_i, the lines tangent to the points where the source crosses the speed of sound in the view of figure 3. Figure 11 clarifies the reason for this: just because our potential ϕ which is (eventually) constant along the characteristics of (9), is a well-behaved function of θ, smooth and with finite derivatives, does not mean that ϕ is also a well-behaved function of the $\xi_\pm$ coordinates normal to these characteristics. On the contrary: the relation between θ and ξ introduces an arccos function when we represent ϕ in terms of ξ, which gives rise to a divergent derivative. For the solution (24), we have $2\phi(\xi) = \Phi_0(\theta_1 - \arccos(\xi/r_s))$:

$$\frac{\partial}{\partial\xi}\phi = \frac{1}{2}\frac{\Phi_0'\left(\theta_1 - \arccos\left(\frac{\xi}{r_s}\right)\right)}{r_s\sqrt{1-\frac{\xi^2}{r_s^2}}} \tag{34}$$

which diverges at $\xi = r_s$ unless $\Phi_0'(\theta_1) = 0$. For the second solution (30), we have $\phi(\xi) = \frac{-r_s}{2\varepsilon_0 cP}\int_{-\theta_1}^{\theta_1 - \arccos(\xi/r_s)} D_n(\theta)d\theta$:

$$\frac{\partial}{\partial\xi}\phi = \frac{-r_s}{2\varepsilon_0 cP}\frac{D_n\left(\theta_1 - \arccos\left(\frac{\xi}{r_s}\right)\right)}{r_s\sqrt{1-\frac{\xi^2}{r_s^2}}} \tag{35}$$

which diverges at $\xi = r_s$ unless $D_n(\theta_1) = 0$.

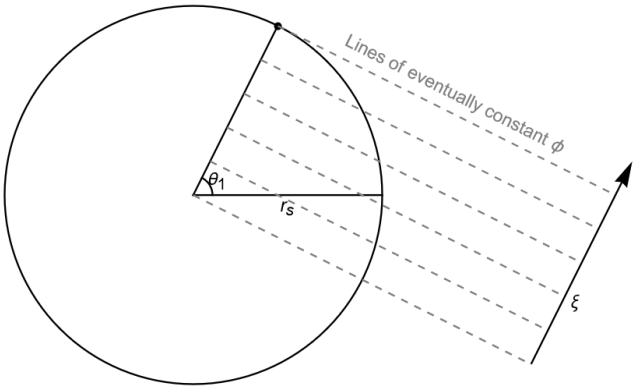

FIG. 11. The relation between ϕ expressed as function of θ along the source boundary, and ϕ expressed as function of ξ, introduces an arccosine function, yielding divergent derivatives w.r.t. ξ even when ϕ is well-behaved as function of θ.

I. A note on regularity

Consider the function

$$f(x,y) = \frac{2(x-1)y}{(x-1)^2+y^2} + y \tag{36}$$

Note

$$f(\cos(\theta),\sin(\theta)) = 0 \tag{37}$$

$$\frac{\partial}{\partial\theta} f(\cos(\theta),\sin(\theta)) = 0 \tag{38}$$

But

$$\frac{\partial}{\partial y} f(1,y) = 1 \tag{39}$$

The derivative along the $r = 1$ circle does not equal the derivative along the $x = 1$ tangent line, not even at the point (1,0) where this line is tangent to this circle.

Both solutions (24) and (30) have this property. Recalling our parameterization of the tangent lines (19), for the first kind of solution (24) we get

$$\phi_0(L_i(\delta)) = \Phi_0(\theta_i) + \frac{\delta}{2r_s}\Phi_0'(\theta_i) + O(\delta^2) \tag{40}$$

The derivative along the circle is $\Phi_0'(\theta)$. For the second kind of solution (30),

$$\phi_1(L_i(\delta)) = \frac{-\delta}{2\varepsilon_0 cP} D_n(\theta_i) + O(\delta^2) \tag{41}$$

The derivative along the circle is 0.

J. Power flow and radiation at infinity

Consider, for either solution, the resonance cone launched in the first quadrant. Far enough from the source, the potential takes the form $\phi = f(\xi_+)$. Following Colas[7], we obtain an approximation for $\boldsymbol{H}$ from Ampère's law

$$\nabla\times\boldsymbol{H} = i\varepsilon_0\omega_0\varepsilon\nabla\phi \tag{42}$$

$$\nabla\times\boldsymbol{H} = \frac{i\varepsilon_0\omega_0}{\sqrt{c^2+1}}\begin{bmatrix} -Sf'(\xi_+) \\ -iDf'(\xi_+) \\ cPf'(\xi_+)\end{bmatrix} \tag{43}$$

Supposing that $\boldsymbol{H}$ also depends only on ξ_+,

$$\begin{bmatrix} -cH_y'(\xi_+) \\ cH_x'(\xi_+)+H_z'(\xi_+) \\ -H_y'(\xi_+)\end{bmatrix} = i\varepsilon_0\omega_0\begin{bmatrix} -Sf'(\xi_+) \\ -iDf'(\xi_+) \\ cPf'(\xi_+)\end{bmatrix} \tag{44}$$

The component of the Poynting vector that is of interest, the component along the cone, i.e. along $(\cos(\theta_2-\pi/2),0,\sin(\theta_2-\pi/2))$, depends only on H_y. The x and z components of (44) are not linearly independent, so we may solve either one

$$H_y'(\xi_+) = \frac{i\varepsilon_0\omega_0 S}{c} f'(\xi_+) \tag{45}$$

The Poynting vector component along the cone is

$$-\frac{1}{2}H_y(\xi_+)^* f'(\xi_+) \tag{46}$$

Integration by parts will now give us the total power that radiates along the cone. Assuming $H_y = 0$ outside the cone,

$$\int_{-r_s}^{r_s} -\frac{1}{2}H_y(\xi_+)^* f'(\xi_+) d\xi_+ \tag{47}$$

$$= -\int_{-r_s}^{r_s} -\frac{1}{2}H_y'(\xi_+)^* f(\xi_+) d\xi_+ \tag{48}$$

$$= \frac{i\varepsilon_0\omega_0 S}{2c}\int_{-r_s}^{r_s} f'(\xi_+)^* f(\xi_+) d\xi_+ \tag{49}$$

This finite quantity is the time-averaged power flow along the cone:

$$\Re\left(\frac{i\varepsilon_0\omega_0 S}{2c}\int_{-r_s}^{r_s} f'(\xi_+)^* f(\xi_+) d\xi_+\right) \tag{50}$$

Considering again a mode $\exp(im\theta)$ on the source boundary (either for e_θ or for D_n), (50) is positive (power flow from the source to infinity) for positive m, and negative for negative m (power flow from infinity to the source). Purely real solutions, such as the example from section III A, or the $m = 0$ mode from figure 10, are standing waves with no associated power flow.

IV. FIELD SINGULARITIES WITHOUT THE ELECTROSTATIC APPROXIMATION

Leaving the electrostatic approximation for now, we can reach the same conclusion, regarding the existence and location of singular electric fields, emitted from the roots of $S\cos^2(\theta)+P\sin^2(\theta) = 0$, directly in the electromagnetic

case. Consider a point on a generic smooth surface, with a surface normal $\boldsymbol{n}$. Consider a Cartesian coordinate system, take the magnetic field as usual along the z axis, and rotate the coordinate system around z such that $\boldsymbol{n}$ is in the xz plane: $\boldsymbol{n} = (\cos(\theta), 0, \sin(\theta))$ for some θ. The two directions tangential to the surface are $\boldsymbol{t}_1 = (-\sin(\theta), 0, \cos(\theta))$ and $\boldsymbol{t}_2 = (0,1,0)$. The surface charge density $\sigma_s = D_n = \boldsymbol{n} \cdot \varepsilon_0 \boldsymbol{\varepsilon} \boldsymbol{E}$ then relates to $e_n = \boldsymbol{n} \cdot \boldsymbol{E}$, $e_1 = \boldsymbol{t}_1 \cdot \boldsymbol{E}$, and $e_2 = \boldsymbol{t}_2 \cdot \boldsymbol{E}$ as

$$\begin{aligned} \frac{\sigma_s}{\varepsilon_0} &= e_n \left(S\cos^2(\theta) + P\sin^2(\theta) \right) \\ &\quad + e_1 (P - S)\sin(\theta)\cos(\theta) \\ &\quad + iDe_2 \cos(\theta) \end{aligned} \tag{51}$$

We see the factor $1/(S\cos^2(\theta) + P\sin^2(\theta))$ appear in the expression for e_n, and θ has the same interpretation as in 2D: the angle between the surface normal and the confining magnetic field is $\pi/2 - \theta$. Even with a finite tangential electric field, and a finite surface charge density, the sign difference between S and P allows e_n to be singular at the roots of $S\cos^2(\theta) + P\sin^2(\theta)$. The presence of this factor strongly suggests that our observations from the 2D electrostatic case generalize to the 3D electromagnetic case, leaving open only the remote possibility that $\frac{\sigma_s}{\varepsilon_0} - e_1(P-S)\sin(\theta)\cos(\theta) - iDe_2 = 0$ when $P\sin^2(\theta) + S\cos^2(\theta) = 0$, in which case the singularity cancels.

V. CONCLUSION

The presence of the electric field singularity at the points where the source surface is tangent to the cone, and everywhere along the cone that connects to those points, explains why many authors who attempted to numerically model the sources in geometric detail[8–10] (as opposed to imposing smooth initial conditions along a coordinate plane) concluded that substantial collision-like losses must be introduced to render the problem numerically solvable (often requiring far more losses than is physically plausible). As already shown in figure 1, introducing such losses does regularize the Green's function of the 3D problem (i.e. of the 2D time-domain wave equation), though it does not shed much light on the numerically crucial problem of determining a characteristic thickness of the cone. The time-domain wave equation (5) is scale-invariant: it is possible to rescale "space" (x, y) and "time" (z) such that the equation remains the same. This is related to Bellan's observation[2] that the dispersion relation of the resonance cone depends only on the angle between the magnetic field and the wavevector, but not on the norm of the wavevector: in the electrostatic, homogeneous, cold, collisionless approximation, there is no physical length scale encoded in the physics of this problem. This scale-invariance is not removed by the introduction of collisions. Removing it may require warm plasma corrections.

We have derived, for the first time, the general exact solution for the potential of the resonance cone emitted by a convex source with finite, non-singular, surface sources, in 2D in the cold, homogeneous, electrostatic approximation. We have given an expression for the power that radiates from such a source in the form of resonance cones. We have shown where, on general curved source surfaces, in 2D or 3D, resonance cones are emitted (i.e. where the associated electric field is singular). An understanding of where the resonance cones are emitted, and what the mathematical description of the singularity is in a neighborhood of these emission points, may lead to the ability to model resonance cones accurately, even using finite element methods which usually do not handle singularities well.

The authors have no conflicts to disclose. Data sharing is not applicable to this article as no new data were created or analyzed in this study.

[1] T. H. Stix, *Waves in plasmas* (Springer Science & Business Media, 1992).
[2] P. M. Bellan, *Fundamentals of plasma physics* (Cambridge university press, 2008).
[3] M. Brambilla, *Kinetic theory of plasma waves: homogeneous plasmas*, 96 (Oxford University Press, 1998).
[4] J. R. Myra and D. A. D'Ippolito, "Resonance cone interaction with a self-consistent radio-frequency sheath," Phys. Rev. Lett. **101**, 195004 (2008).
[5] V. Maquet, A. Druart, and A. Messiaen, "Analytical edge power loss at the lower hybrid resonance: comparison with ANTITER IV and application to ICRH systems," arXiv preprint arXiv:2101.09503 (2021).
[6] W. Tierens, J. Myra, R. Bilato, and L. Colas, "Resonant wave–filament interactions as a loss mechanism for HHFW heating and current drive," Plasma Physics and Controlled Fusion **64**, 035001 (2022).
[7] L. Colas, W. Tierens, J. Myra, and R. Bilato, "Radio-frequency sheath excitation at the extremities of scrape-off layer plasma filaments, mediated by resonant high harmonic fast wave scattering," Journal of Plasma Physics **88**, 905880614 (2022).
[8] W. Zhang, R. Bilato, V. V. Bobkov, A. Cathey, A. Di Siena, M. Hoelzl, A. Messiaen, J. R. Myra, G. S. López, W. Tierens, *et al.*, "Recent progress in modeling ICRF-edge plasma interactions with application to ASDEX upgrade," Nuclear Fusion (2021).
[9] L. Lu, *Modelling of plasma-antenna coupling and non-linear radio frequency wave-plasma-wall interactions in the magnetized plasma device under ion cyclotron range of frequencies*, Ph.D. thesis, Université de Lorraine (2016).
[10] F. Paulus, *Studies of propagating slow waves in the ion cyclotron range of frequencies (in preparation)*, Ph.D. thesis, Ludwig-Maximilians-Universität (2023).
[11] R. K. Fisher and R. W. Gould, "Resonance cones in the field pattern of a radio frequency probe in a warm anisotropic plasma," The Physics of Fluids **14**, 857–867 (1971), https://aip.scitation.org/doi/pdf/10.1063/1.1693521.